ELSEVIER

PII: S0032-3861(96)01071-3

Polymer Vol. 38 No. 15, pp. 3985–3989, 1997

0032-3861/97/$17.00 + 0.00

polymer communications

N.m.r. imaging of the diffusion of water into poly(tetrahydrofurfuryl methacrylate-*co*-hydroxyethyl methacrylate)

P. Y. Ghi and D. J. T. Hill*
Department of Chemistry, University of Queensland, QLD 4072, Australia

and D. Maillet and A. K. Whittaker
Centre for Magnetic Resonance, University of Queensland, QLD 4072, Australia
(Received 3 December 1996)

Nuclear magnetic resonance (n.m.r.) imaging was used to study the ingress of water into poly(tetrahydrofurfuryl methacrylate-*co*-hydroxyethyl methacrylate). The study offers strong evidence that the diffusion is Fickian in nature. The diffusion coefficient, D, obtained by fitting the underlying diffusion profile, attainable from the images, according to the equation for Fickian diffusion, is 1.5×10^{-11} m^2 s^{-1}, which is in good correlation with the value of 2.1×10^{-11} m^2 s^{-1}, obtained from mass uptake measurements. Additionally, from the T_2-weighted images, superimposed features observed in addition to the underlying Fickian diffusion profiles were shown to have a longer spin–spin relaxation time, T_2. This suggests the presence of two types of water within the polymer matrix; a less mobile phase of absorbed water that is interacting strongly with the polymer matrix and a more mobile phase of absorbed water residing within the cracks observed in the environmental scanning electron micrograph. © 1997 Elsevier Science Ltd.

(Keywords: methacrylate polymers; n.m.r. imaging; Fickian diffusion)

Introduction

Methacrylate polymers are widely applied in biomedicine because of their established biocompatibility[1]. The general chemical structure for a methacrylate polymer is shown in *Figure 1*, in which the R group may be replaced by a number of substituents, offering polymers of varied properties.

The polymers under investigation in this paper swell in an aqueous environment and are applicable as controlled drug delivery systems. When an initially glassy swellable polymeric matrix, with a drug uniformly dispersed in it, is placed in water, the polymer begins to swell as the water penetrates the matrix. This results in the subsequent diffusion of the drug from the swollen polymer matrix into the surroundings. In a release system controlled by swelling, the kinetics of release of the incorporated drug is determined by the rate of diffusion of the aqueous medium into the system.

The kinetics of diffusion in polymers, range from simple Fickian diffusion to higher order diffusion, such as Case II diffusion[4,5]. Fickian diffusion is characterized by a mass uptake that is proportional to the square root of diffusion time, whereas Case II diffusion is characterized by a mass uptake that is directly proportional to time. The conventional method for determining the characteristics of diffusion of solvents into polymer matrices is by measuring the mass uptake of the polymer as the solvent penetrates the matrix. However, since such measurements entail observations at a macroscopic level, little information has been obtained relating to the nature of the solvent in the polymer matrix and the mechanisms of the processes which control its diffusion. The method also suffers from a reliance on a model for the diffusion process since the nature of the absorption profile is not observed directly.

Nuclear magnetic resonance (n.m.r.) imaging has recently been used to observe the ingress of solvents into solid systems[6–8]. The method provides a two- or three-dimensional image of the density of the highly mobile component in a material. The principal advantage of the technique is the possibility of visualizing the diffusion profile, the concentration and location of the permeating liquid in a solid sample, hence making it possible to determine diffusion coefficients. The form of the diffusion profile can be related to the type of diffusion that is occurring within the polymer. Fickian diffusion is characterized by a diffusion profile that decreases gradually from the swollen, rubbery region to the glassy polymer core, whereas Case II diffusion has two definitive characteristics. The diffusion profile maintains a constant water content within the outer rubbery region and exhibits a sharp decrease in water content from the boundary of the rubber/glass interface to the inner glassy region[9]. In addition, it should be noted that the rate of advance of the diffusion front is proportional to the square root of time for Fickian diffusion, but proportional to time for Case II diffusion.

Patel and coworkers have, for several years, been involved in the development of delivery systems based on heterocyclic methacrylates with a potential for use in dentistry. They have developed a system consisting of poly(tetrahydrofurfuryl methacrylate), PTHFMA, in the form of an interpenetrating polymer network (IPN) with poly(ethyl methacrylate), PEMA, that has found application in dentistry as a material for temporary crown and bridge amalgams[10]. The system possesses such favourable properties as ease of fabricaton, excellent biological

* To whom correspondence should be addressed

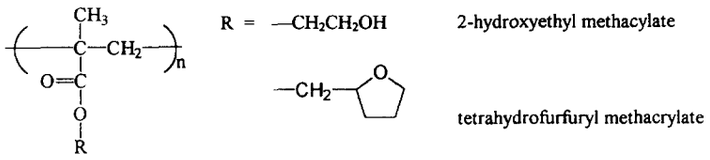

Figure 1 Chemical structure of the methacrylate polymer used in this study

tolerance[11] and reasonable mechanical performance[12]. Perhaps the most important property of PTHFMA is its ability to absorb water[13], capable of facilitating the release of bio-active materials by diffusion out of the swollen polymer matrix. The rate of water absorption, as determined by mass uptake measurements, into PTHFMA and THFMA-based systems have been reported to exhibit anomalous behaviour[13] (a combination of Fickian and Case II diffusion).

The aim of this paper is to investigate the processes which control the diffusion of water in methacrylate-based polymer systems used for the controlled release of bio-active materials. The system studied is a copolymer of tetrahydrofurfuryl methacrylate and 2-hydroxyethyl methacrylate (HEMA). The incorporation of a hydrophilic component by copolymerization increases the rate of diffusion of water and offers the opportunity to control the rate of diffusion of water by varying the copolymer composition. Additionally, since Wichterle and Lim[14] first proposed the use of PHEMA in contact lenses, PHEMA has become a common ingredient in medical formulations because of its high degree of chemical stability and mechanical integrity.

Experimental

The method of purification of the monomers, THFMA and HEMA, and the initiator, benzoyl peroxide, used for the synthesis of the copolymer has been previously described[15]. After purification, the required amounts of the monomers and the initiator were prepared in 25 ml volumetric flasks, giving an initiator concentration of 0.05 M in the monomers. The copolymer contains a molar ratio of 1/9 of THFMA/HEMA. The solution was subsequently transferred to cylindrical teflon moulds and polymerized under a nitrogen atmosphere at $40 \pm 2°C$ for the first 3 h of the 24-h reaction period, followed by 3 h at $60 \pm 2°C$ and at $80 \pm 2°C$ for the remaining reaction time. The samples are transparent cylinders with dimensions, 1 cm × 3 cm (diameter × length). There was negligible change in the dimension of the cylinder during the absorption of the water.

The copolymer in the form of a cylinder was immersed in distilled water at 298 K. The polymer was removed at various time intervals and n.m.r. images of the polymer were obtained using a Bruker AMX400 spectrometer. Images were acquired using the spin-echo three-dimensional pulse sequence, with a 90° pulse of duration 50 μs and an echo and recovery time of 2.4 ms and 2.0 s, respectively. The strength of the read gradient was $0.08\ T\ m^{-1}$ and the image consisted of 256 × 256 × 8 voxels. Two averages were co-added giving a total acquisition time of 2 h. The images of the diffusion profiles were obtained in the central region of the cylinder.

Environmental scanning electron microscopy (ESEM) experiments were performed on an Electroscan ESEM operating at an electronic discharge of 7 keV.

Results and discussion

Poly(THFMA-*co*-HEMA) was immersed in water and periodically removed to monitor the increase in mass as water was incorporated into the polymer matrix. *Figure 2* is a plot of the mass increase of the copolymer as a function of the square root of time. The plot is linear up to 48 h, suggesting the occurrence of Fickian diffusion. A numerical fit of experimental data to the Fickian equation[4] for diffusion gives a diffusion coefficient of $1.2 \times 10^{-11}\ m^2\ s^{-1}$. The equation[4] used is the solution to Fick's second law for diffusion into an infinite cylinder where transfer occurs only in the radial direction:

$$\frac{M_t}{M_\infty} = 1 - \sum_{n=1}^{\infty} \frac{4}{\beta_n^2} \exp\left(\frac{-D\beta_n^2 t}{a^2}\right) \qquad (1)$$

where M_t is the mass of water at time, t; M_∞ is the mass of water at infinite time; a is the radius of the cylinder; D is the diffusion coefficient; and β_n are the roots of the zero order Bessel function $J_0(\beta_n) = 0$. Simulation of the mass–time curve required a summation over 150 roots.

N.m.r. imaging experiments for poly(THFMA-*co*-HEMA) were performed in parallel with mass uptake measurements. *Figure 3* shows the concentration of water in the polymer matrix across the diameter of the cylinder, at the various time intervals up to 48 h of immersion in water. Two features are discernible from the profiles. The underlying profile is indicative of simple Fickian diffusion, as shown by the numerical fit to the Fickian equation[4] of diffusion. The equation used for the

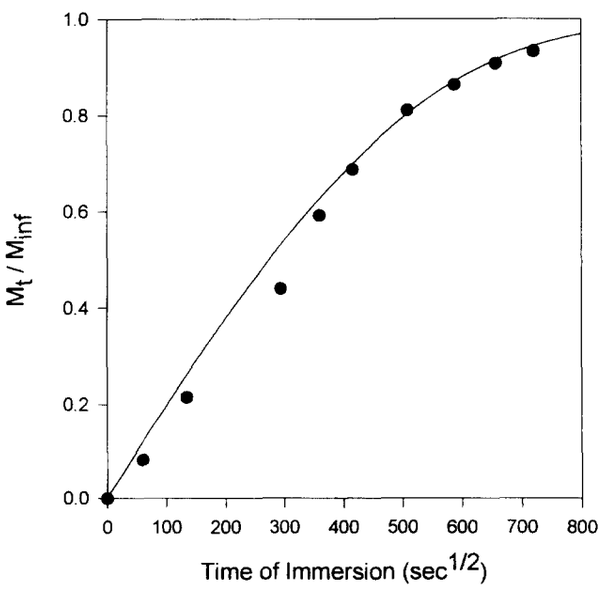

Figure 2 Mass increase vs. square root of immersion time for poly(THFMA-*co*-HEMA). Mole fraction of THFMA/HEMA is 1/9. ●, Experimental data; —, theoretical fit based on Fickian diffusion. $D = 2.1 \times 10^{-11}\ m^2\ s^{-1}$

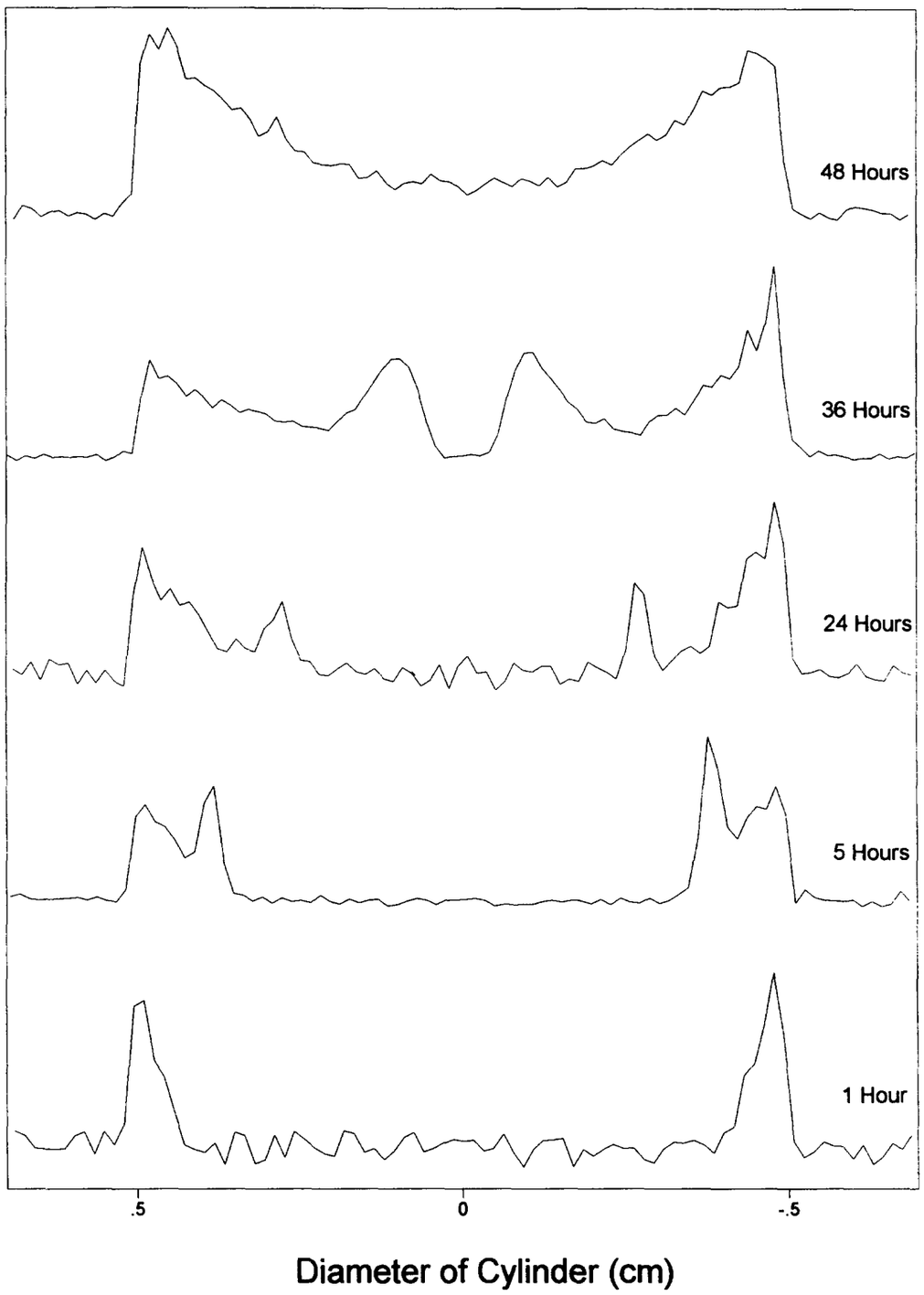

Figure 3 Water–concentration profiles at various immersion times for poly(THFMA-*co*-HEMA). Mole fraction of THFMA/HEMA is 1/9

numerical fit is:

$$\frac{C_r}{C_\infty} = 1 - 2\sum_{n=1}^{\infty} \frac{J_0(r\beta_n/a)}{\beta_n J_1(\beta_n)} \exp\left(-D\frac{\beta_n^2}{a^2}t\right) \qquad (2)$$

where C_r is the concentration at distance, r, into the cylinder and C_∞ is the concentration of water at the surface of the cylinder and J_0 and J_1 are Bessel functions of the zero and first order, respectively. The diffusion coefficient obtained from the fit, using a summation over 100 roots, is 1.5×10^{-11} m^2 s^{-1}, which is in approximate agreement with the value obtained from the mass uptake measurements. The larger value of the diffusion coefficient obtained from the mass uptake experiments can be attributed to end effects that are ignored in equation (1), which applies for an infinite cylindrical rod. The experimental profile for 48 h diffusion and the numerical fit to this data are shown in *Figure 4*.

Closer examination of the profiles, obtained at shorter diffusion times, revealed superimposed features closer to the diffusion front that are inconsistent with Fickian diffusion. N.m.r. images acquired at two different echo times (T_2-weighted images) directly affected the intensity of the two features observed in the profiles. The water–concentration profiles from the T_2-weighted images are given in *Figure 5*. The two features (the underlying

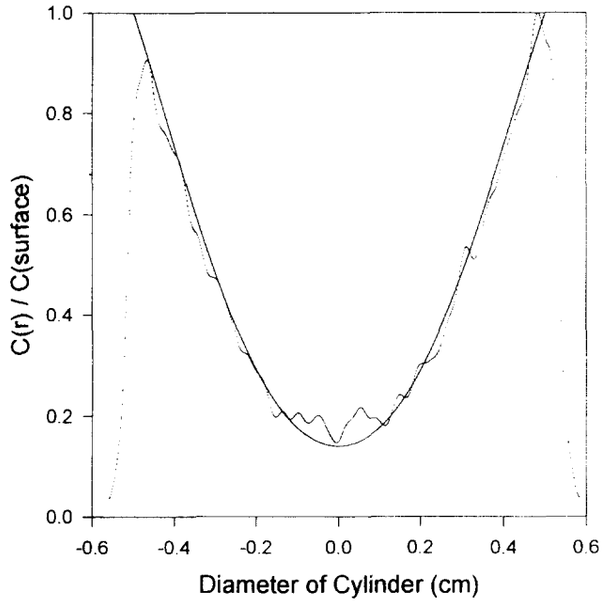

Figure 4 Water–concentration profile for poly(THFMA-*co*-HEMA) after 48 h immersion in water. Mole fraction of THFMA/HEMA is 1/9. . . ., Experimental profile obtained from an n.m.r. image; —, theoretical fit based on Fickian diffusion. $D = 1.5 \times 10^{-11}\ m^2\ s^{-1}$

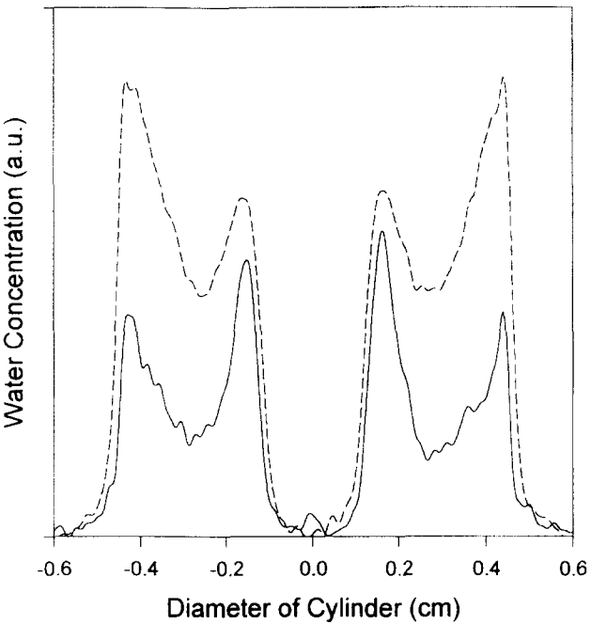

Figure 5 Relaxation time-weighted profiles at two echo times for poly(THFMA-*co*-HEMA) after 24 h immersion in water. Mole fraction of THFMA/HEMA is 1/9. —, Echo time = 5.56 ms; – –, echo time = 3.76 ms

Fickian feature and the superimposed feature) exhibit a disproportionate decrease in intensity as the echo time is increased, indicating the presence of two types of absorbed water in the polymer matrix. The two different phases are a less mobile phase (short T_2) that is interacting strongly with the polymer matrix and contributing to the underlying Fickian profile and a more mobile phase (long T_2) confined to a narrow annular region that has penetrated deeper into the polymer matrix. The presence of defects in the polymer matrix, such as cracks, may explain for the existence of the more mobile phase of absorbed water within the polymer. Stress-related crack formation, as a result of solvent diffusion has been observed in systems exhibiting Case II diffusion[5,16].

The surface morphology of the copolymer was investigated by ESEM. ESEM is an ideal technique to observe the surfaces of polymers swollen with a liquid, since the sample can be maintained in the wet stage and at low pressure during a scan. *Figure 6* shows the ESEM micrograph of the surface of the copolymer around the region of low water content, taken after being immersed in water for 24 h. The micrograph clearly shows a network of cracks. As the polymer absorbs water, stress is created since a rubbery region now exists within the initially glassy polymer. Stress formation is then capable of initiating crack development. Therefore, it can be concluded that the more mobile phase of absorbed water detected in the T_2-weighted images are water molecules residing in the observed cracks.

The existence of cracks within the polymer provides an alternative route for the transfer of water within the polymer. This is one reason for the larger value of the diffusion coefficient obtained from mass uptake measurements in comparison to the smaller value obtained from the n.m.r. image, since the former method measures a macroscopic quantity that reflects an overall contribution to the transfer process (the absorption of water in the radial and longitudinal direction and the transfer of water through the crack channels). N.m.r. imaging is a more accurate technique of characterizing the diffusion process since the different modes of transfer may be differentiated and hence analysed separately.

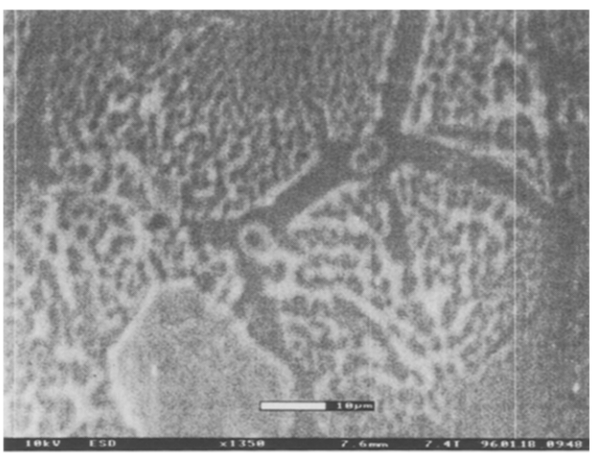

Figure 6 ESEM micrograph of poly(THFMA-*co*-HEMA) after 24 h immersion in water. Mole fraction of THFMA/HEMA is 1/9. Surface image across the base of the cylinder at the region of low water content

Conclusions

N.m.r. imaging has been demonstrated to be an invaluable tool for the characterization of diffusion of water into poly(THFMA-*co*-HEMA). Water–concentration profiles were directly observable and the experiments performed at various immersion times allowed the visualization of the mechanism of diffusion in the system. Additionally, the acquisition of T_2-weighted images shows that there are two types of absorbed water in the polymer matrix. These are: (1) the less mobile phase that is interacting strongly with the matrix and contributing to the underlying Fickian profile; (2) a more mobile phase

that exists within cracks. These cracks were directly observed in the ESEM micrographs and are the result of stress formation during the diffusion process.

Acknowledgements

The authors would like to acknowledge Dr Patel, Prof. Braden and Prof. Anseau of the London Hospital Medical College, for helpful discussions and input into this project. They also wish to acknowledge financial support from the Australian Reseach Council.

References

1. Ridley, H., *Trans. Ophthalmol. Soc. UK*, 1952, **71**, 617.
2. Ratner, B. D. and Hoffman, A. S., in *Synthetic Hydrogels for Biomedical Applications*, Vol. 31, ed. J. D. Andrade, Hydrogels for Medical and Related Applications, ACS Symposium Series. American Chemical Society, Washington DC, 1976, pp. 1–36.
3. Langer, R., *Rev. Macromol. Chem. Phys.*, 1983, **C23**(1), 61.
4. Crank J. and Park, G. S., *Diffusion in Polymers*, 1st edn. Academic Press, New York, 1968.
5. Alfrey, A., Gurnee, E. F. and Lloyd, W. G., *J. Polym. Sci.*, 1966, **C12**, 249.
6. Webb, A. G. and Hall, L. D., *Polymer*, 1991, **32**, 422.
7. Grinsted, R. A. and Koenig, J. L., *Macromolecules*, 1992, **25**, 1229.
8. Hyde, T. M., Gladden, L. F., Mackley, M. R. and Gao, P., *J. Polym. Sci., A, Polym. Chem.*, 1995, **33**, 1795.
9. Weisenberg, L. A. and Koenig, J. L., *Appl. Spectroscopy*, 1989, **43**, 1117.
10. Ibsen, R. L. and Glace, W. R., European Patent No. 0032249, 1984.
11. Pearson, G. J., Picton, D. C. A., Braden, M. and Longman, C., *Int. End. J.*, 1986, **19**, 121.
12. Patel, M. P. and Braden, M., *Biomaterials*, 1991, **12**, 645.
13. Patel, M. P. and Braden, M., *Biomaterials*, 1991, **12**, 653.
14. Wichterle, O. and Lim, D., *Nature*, 1960, **185**, 117.
15. Ghi, P. Y., Hill, D. J. T., Pomery, P. J. and Whittaker, A. K., *Polymer Gels and Networks*, 1996, **4**(3), 253.
16. Hopfenberg, H. B., Holley, R. H. and Stannett, V., *Polym. Eng. Sci.*, 1968, **9**, 242.